Theoretical Study of Hydration of Cyanamide and Carbodiimide

**Francesco Tordini,[†] Alessandro Bencini,[‡] Maurizio Bruschi,[§] Luca De Gioia,[†]
Giuseppe Zampella,[†] and Piercarlo Fantucci*,[†]**

*Department of Biotechnology and Biosciences, University of Milano-Bicocca, Piazza della Scienza 2,
I-20156 Milan, Italy, Department of Chemistry, University of Florence, Via Maragliano 75-77,
I-50144 Florence, Italy, and Department of Environmental Sciences, University of Milano-Bicocca,
Piazza della Scienza 1, I-20156 Milan, Italy*

Received: July 16, 2002; In Final Form: November 27, 2002

The isomerization reaction cyanamide → carbodiimide in vacuo and in the presence of up to six water molecules has been investigated by means of DFT and MP2 calculations, using a flexible basis set. The reliability of such methods has been checked against results of coupled cluster calculations on isolated molecules. The effect of water molecules has also been investigated in the case of the hydrolysis reaction of cyanamide and carbodiimide, leading to isourea. The number of water molecules considered is large enough to give results converged in activation and hydration energies. In addition to the water molecules explicitly described, the effect of water bulk solvent is taken into account according to the polarizable continuum model. The results show that the direct hydrolysis of H_2NCN is hindered by an activation energy much higher than that for HNCNH, which in turn can be obtained from cyanamide with a relatively easy process.

Introduction

Cyanamide [$H_2N-C\equiv N$; **a**] and its tautomer carbodiimide [$HN=C=NH$; **b**] are important molecules entering several chemical processes. Cyanamide is an intermediate in synthesis of pharmaceuticals, pesticides, herbicides, and various polymers,[1] and it is also assumed to be relevant in prebiotic chemistry.[2] Carbodiimides are important reagents for peptides and nucleotide synthesis.[3]

Reactions of cyanamide and carbodiimide usually occur via nucleophilic attack to the carbon atom; for istance, a water molecule acting as a nucleophile, leads to urea. A similar behavior is present also in bio-processes, as shown by recent studies on carbonic anhydrase isozymes I (HCAI) and II (HCAII),[4,5] where, in addition, cyanamide acts also as a potent suicide substrate.[6]

The understanding of the hydration mechanism of **a** and **b** within the enzyme[7] would be very useful for designing potent inhibitors. However, very little is known about the mechanism occurring at the active site of the HCA which could be, partly, cleared by investigation of the behavior of the two isolated tautomers.

Cyanamide and carbodiimide have been extensively studied in the past,[8] both theoretically and experimentally, as for their equilibrium structures,[9−12] torsional-rotational dynamics,[9] and IR frequencies.[11] On the contrary, to our knowledge, tautomerization and hydrolysis of **a** have never been studied theoretically. The hydration of **b** has been recently investigated by Nguyen et al.[13] and Glaser et al.,[14] who pointed out that a second actively involved water molecule plays also a role in the mechanism. Even a third water molecule, not directly involved in the proton transfer, can further contribute to the kinetics.[14] To complete the theoretical study of the reactivity of **a** and **b** with water, we carried out a detailed investigation of the following reactions:

$$H_2N-C\equiv N \rightarrow HN=C=NH \qquad (1)$$

$$H_2N-C\equiv N + H_2O \rightarrow H_2NCONH_2 \qquad (2)$$

$$HN=C=NH + H_2O \rightarrow H_2NCONH_2 \qquad (3)$$

considered in a vacuum as well as in the presence of water clusters $(H_2O)_n$ ($n = 1-6$) explicitly described and bulk solvent simulated by the polarizable continuum model (PCM). The aim of our study is (i) to compare the performance of various theoretical methodologies in predicting molecular properties of **a** and **b**, and energetics of the **a** → **b** interconversion; (ii) to investigate the cooperative effect of water molecules in the hydrogen transfer from **a** to **b**; and (iii) to find the most convenient path for hydrolysis of the two tautomers **a** and **b**.

Computational Methods

Structural parameters and stability of cyanamide and carbodiimide in energy minima and at transition states (TS) have been computed with MP2[15] and CCSD[16] ab initio methods and with several density functional theory (DFT)[17] pure and hybrid exchange-correlation functionals. The MP2, CCSD, and DFT calculations have been carried out using the split valence basis set augmented by a full set of polarization functions, 6-31G-(d,p).[18] In the case of MP2, geometry optimizations have been also performed with the consistent-correlated cc-pVQZ basis set of Dunning.[19] Improved energies of **a** and **b** have been estimated at the CCSD(T)/cc-pVQZ level of theory at MP2/cc-pVQZ optimum geometry.

The effect of water molecules on **a** → **b** isomerization and on hydrolysis of both isomers has been analyzed at DFT-B3LYP[20] and MP2 levels only. Searches of stationary points

---

* To whom correspondence should be addressed. E-mail: piercarlo.fantucci@unimib.it. Phone: +39-02-64483477. Fax: +39−02−64483478.

[†] Department of Biotechnology and Biosciences, University of Milano-Bicocca.

[‡] University of Florence.

[§] Department of Environmental Sciences, University of Milano-Bicocca.

10.1021/jp026535r CCC: $25.00

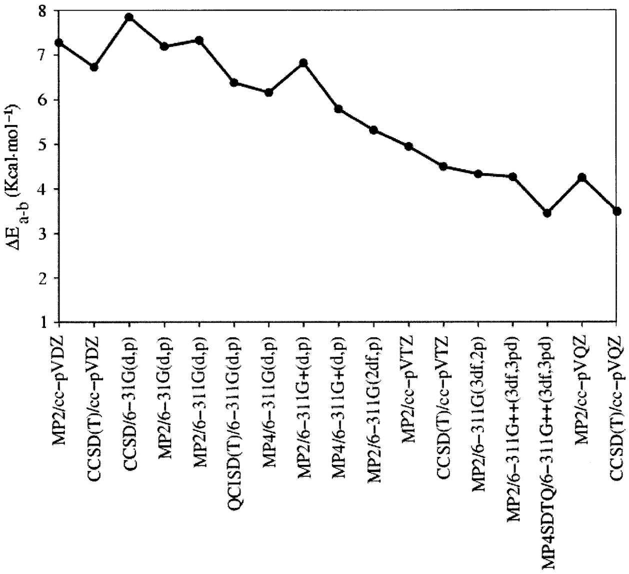

Figure 1. Dependence of **a** → **b** isomerization energy on the extent of electron correlation and basis set size.

of the potential energy have been performed by gradient-based algorithms and by synchronous transit guided quasi-newton (STQN) method.[21] The exact nature of each null-gradient point has been checked by vibrational analysis.

Bulk solvent effects are described by the polarizable continuum model (PCM).[22] A possible occurrence of basis set superposition error (BSSE)[23] has been checked in some selected cases (see the Discussion section). The natural atomic orbital (NAO) scheme[24] has been used for charge population analysis.

To overcome the difficulties caused by the lack of experimental data on the energetics of cyanamide and carbodiimide and for a better definition of the reliability of the adopted computational schemes, the energies of **a** and **b** have been also computed at Gaussian-2 (G2) level.[25] All calculations have been performed using the Gaussian 98 suite of programs.[26]

Results

In this section, DFT and MP2 results will be discussed for the process **a** → **b** in vacuo (path **I** of Figure 2) and in the presence of $n = 1, 2, ..., 6$ water molecules. The hydrated forms of **a** and **b** will be labeled **1a**, **2a**, ... and **1b**, **2b**, ... for $n = 1, 2, ...,$ and the corresponding paths will be labeled **I1**, **I2**, ..., respectively. In addition, theoretical results for the hydrolysis of **a** or **b** to isourea (denoted as **c**) will be discussed: the systems corresponding to **a** + $\mathrm{nH_2O}$ → **c** + $\mathrm{(n\text{-}1)H_2O}$ will be denoted shortly as **na** → **nc** (paths **A1**, **A2**, ... for $n = 1, 2, ...$) and the systems **b** + $\mathrm{nH_2O}$ → **c** + $\mathrm{(n\text{-}1)H_2O}$ as **nb** → **nc** (reaction paths **B1**, **B2**, ... for $n = 1, 2, ...$).

Structure and Stability of Cyanamide and Carbodiimide. Equilibrium molecular parameters of **a** and **b** obtained from ab initio and DFT calculations are collected in Tables 1 and 2 and compared with experimental data.[10,12] The results at the B3LYP/6-31G(d,p) calculations are in a fairly good agreement with the experiment, with the exception of the HN- - -NH angle of **b** and the NCN angle of **a** which are in error by about 4°. As for the molecular geometries, DFT compares well with MP2 and CCSD; MP2 reaches an accuracy similar to the B3LYP/6-31G-(d,p) one only when the large cc-pVQZ basis is adopted, and therefore, a larger contribution of correlation is considered. On the other hand, it should be noted (see Table 2) that the discrepancy between theory and experiment seems to be sligthly higher in the case of the B3LYP functional with larger basis.

As for the relative stability of **a** and **b**, the MP2 and CCSD methods, with the 6-31G(d,p) basis, give similar values of the isomerization energy defined as $\Delta E_{\mathbf{a}\to\mathbf{b}} = E(\mathbf{b}) - E(\mathbf{a})$: $\Delta E_{\mathbf{a}\to\mathbf{b}} = 7.2$ and 7.8 kcal mol^{-1} for MP2 and CCSD, respectively. By increasing the basis set size and the amount of the electron correlation, a regular decrease of the computed $\Delta E_{\mathbf{a}\to\mathbf{b}}$ values is observed, as shown in Figure 1. The free energy variation $\Delta G_{\mathbf{a}\to\mathbf{b}}$ obtained by G2 method is equal to 2.5 kcal mol^{-1}, and substantially confirms the CCSD(T)/cc-pVQZ results: $\Delta E_{\mathbf{a}\to\mathbf{b}}$ value of 3.5 kcal mol^{-1} and $\Delta G_{\mathbf{a}\to\mathbf{b}} = 2.4$ and 2.5 kcal mol^{-1}, at 273 and 383 K, respectively, using the Gibbs energy corrections of the G2 method. The latter value is in a fairly good agreement with the experimental value $\Delta G_{\mathbf{a}\to\mathbf{b}} = 3.6$ kcal mol^{-1}.[10]

As for the $\Delta E_{\mathbf{a}\to\mathbf{b}}$ values, ab initio and DFT methods do not completely agree. Indeed, DFT results are very sensitive to the particular exchange-correlation functional and basis set. In the complete absence of HF exchange contribution, **b** seems to be more stable than **a**: $\Delta E_{\mathbf{a}\to\mathbf{b}} < 0$ (see Table 3), whereas hybrid functionals restore the correct order of stability. The B3LYP/6-31G(d,p) $\Delta E_{\mathbf{a}\to\mathbf{b}}$ value is as small as 0.5 kcal mol^{-1}, about 3 kcal mol^{-1} smaller than our best ab initio result: the DFT approaches seem to overestimate the stability of **b**. An unbalanced description in error by about 3 kcal mol^{-1} is probably the limit of DFT approach, which, as pointed out by Parr and Yang,[17] describes with different accuracy molecules with different bond topology, as is the case of HNCNH and $\mathrm{H_2NCN}$.

Mechanism of Cyanamide → Carbodiimide Isomerization. The mechanism of the **a** → **b** reaction has been studied using B3LYP, MP2, and CCSD methods with the 6-31G(d,p) basis set both in vacuo and considering PCM solvent corrections. The reaction involves the transfer of a proton from $\mathrm{N^D}$ (the donor nitrogen atom) to $\mathrm{N^A}$ (the acceptor nitrogen atom, see Scheme 1a). The description of the reaction path and the nature of the TS is very similar for all of the methods adopted (Figure 2, Reaction path **I**). At the TS, the hydrogen atom, which moves from $\mathrm{N^D}$ to $\mathrm{N^A}$, is actually bound to the carbon atom (H−C = 1.17 Å) only, no longer to $\mathrm{N^D}$ and not yet to $\mathrm{N^A}$, and the N−C−N angle is significantly bent (166−168°). The computed activation energy ($\Delta E^{\#}$) is equal to 84.8, 84.0, and 93.8 kcal mol^{-1} for MP2, B3LYP, and CCSD methods, respectively. Such high values suggest that **a** → **b** isomerization, observed in the gas phase, can take place only through a bimolecular mechanism. The $\Delta G^{\#}$ values derived from PCM calculations are very similar (within 1.6 kcal mol^{-1}, see path **I** of Figure 2) to the $\Delta E^{\#}$ values. However, the situation computed in vacuo can change drastically when one or more water molecules are explicitly considered, as in the case of several other reactions involving transfer of polarized hydrogen atoms. Along this line, we carried out PCM-B3LYP/6-31G(d,p) and PCM-MP2/6-31G-(d,p) calculations on **a** and **b** in the presence of up to six water molecules. The structure of the water adducts of cyanamide and carbodiimmide as well as the corresponding TSs are shown in Figure 2. The reaction PCM ΔG values are reported in Figure 2 for the **na** → **TS−In** ($\Delta G^{\#}$ value) and **TS−In** → **nb** steps. For completeness, ΔE values from in vacuo calculations are reported in the caption of Figure 2. The MP2 data will not be commented further, as they follow a trend very parallel to the DFT ones.

The effect of a water molecule is very evident in path **I1** of Figure 2: its activation free energy (36.3 kcal mol^{-1}) is more than 40 kcal mol^{-1} lower than the vacuum value. The TS includes a sort of six-membered ring in which the proton transfer

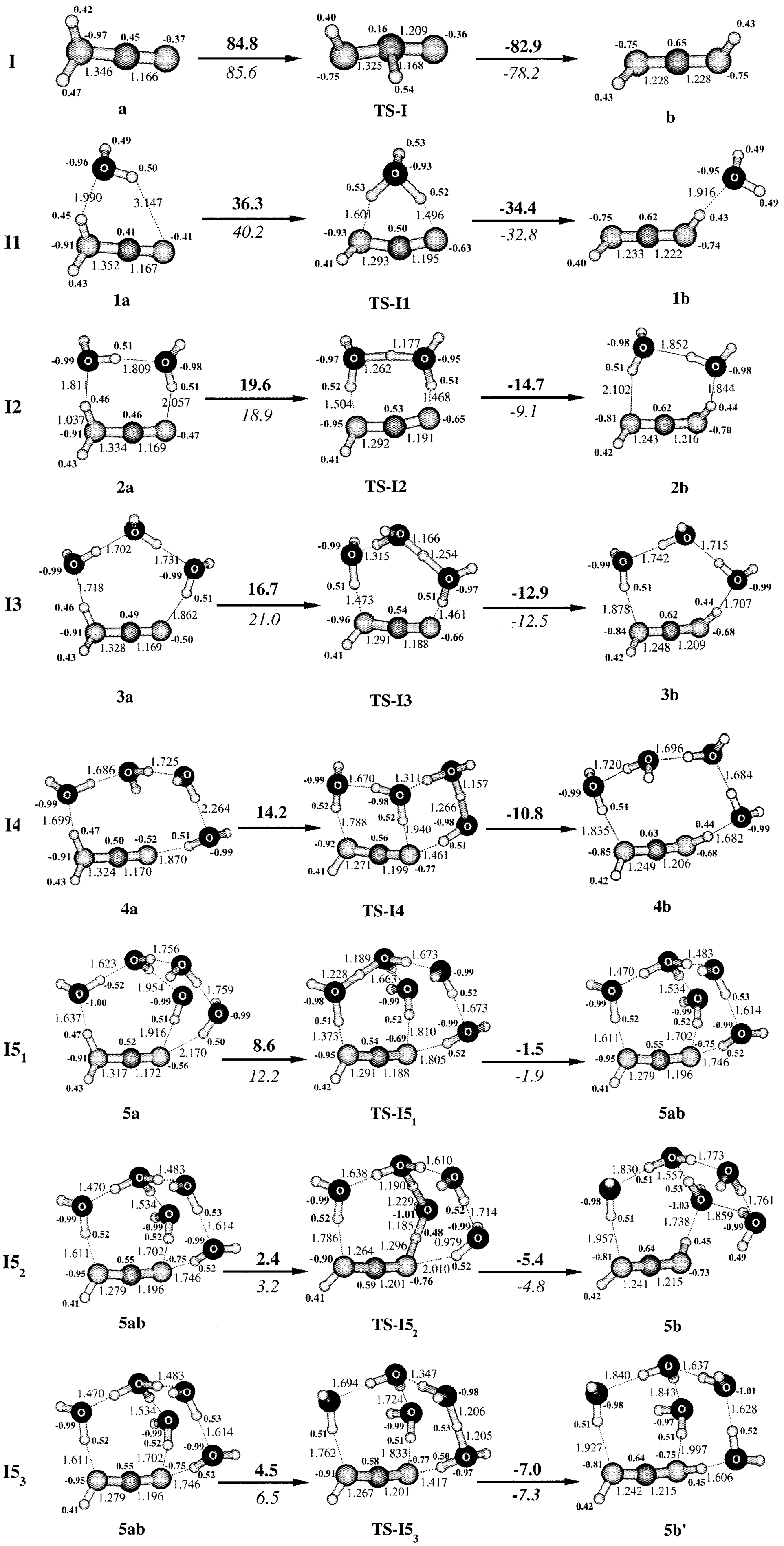
I
0.42 -0.97 0.45 -0.37 1.346 1.166 0.47
a
84.8
85.6
0.40 0.16 1.209 -0.36 -0.75 1.325 1.168 0.54
TS-I
-82.9
-78.2
0.43 -0.75 0.65 1.228 1.228 -0.75 0.43
b
I1
0.49 -0.96 0.50 1.990 3.147 0.45 0.41 -0.41 -0.91 1.352 1.167 0.43
1a
36.3
40.2
0.53 -0.93 0.53 0.52 1.601 1.496 0.50 -0.93 0.41 1.293 1.195 -0.63
TS-I1
-34.4
-32.8
0.49 -0.95 1.916 0.49 -0.75 0.62 0.43 -0.74 0.40 1.233 1.222
1b
I2
-0.99 0.51 -0.98 1.809 1.811 0.51 0.46 2.057 1.037 0.46 -0.91 -0.47 1.334 1.169 0.43
2a
19.6
18.9
1.177 -0.97 -0.95 1.262 0.52 0.51 1.504 1.468 0.53 -0.95 -0.65 1.292 1.191 0.41
TS-I2
-14.7
-9.1
-0.98 1.852 0.51 -0.98 2.102 1.844 0.62 0.44 -0.81 -0.70 0.42 1.243 1.216
2b
I3
1.702 1.731 -0.99 -0.99 1.718 0.51 0.46 0.49 1.862 -0.91 -0.50 0.43 1.328 1.169
3a
16.7
21.0
-0.99 1.166 1.315 1.254 0.51 1.473 0.51 -0.97 0.54 1.461 -0.96 -0.66 0.41 1.291 1.188
TS-I3
-12.9
-12.5
1.742 1.715 -0.99 -0.99 0.51 0.44 1.707 1.878 0.62 -0.84 -0.68 0.42 1.248 1.209
3b
I4
1.686 1.725 -0.99 2.264 1.699 0.47 0.50 -0.52 0.51 -0.91 1.870 -0.99 0.43 1.324 1.170
4a
14.2
-0.99 1.670 1.311 1.157 0.52 -0.98 1.266 1.788 0.52 -0.98 1.940 0.56 -0.92 0.51 1.461 0.41 1.271 1.199 -0.77
TS-I4
-10.8
1.696 1.720 1.684 -0.99 0.51 0.44 1.835 0.63 -0.99 1.682 -0.85 -0.68 0.42 1.249 1.206
4b
$\mathrm{I5}_1$
1.756 1.623 -0.52 -1.00 1.954 -0.99 1.759 1.637 0.51 -0.99 0.47 1.916 0.52 0.50 -0.91 2.170 -0.56 1.317 1.172 0.43
5a
8.6
12.2
1.189 1.673 1.228 -0.99 1.663 -0.98 -0.99 0.52 0.51 0.52 1.673 1.373 1.810 -0.99 0.54 -0.69 -0.95 1.805 0.52 0.42 1.291 1.188
$\mathrm{TS\text{-}I5}_1$
-1.5
-1.9
1.483 1.470 -0.99 1.534 0.53 0.52 -0.99 0.52 1.614 1.611 1.702 -0.75 -0.99 0.55 -0.95 1.746 0.52 0.41 1.279 1.196
5ab
$\mathrm{I5}_2$
1.470 1.483 1.534 -0.99 -0.99 0.53 0.52 1.614 0.52 -0.99 1.611 1.702 0.55 -0.75 -0.95 1.746 0.52 0.41 1.279 1.196
5ab
2.4
3.2
1.638 1.610 -0.99 1.190 1.229 0.52 -1.01 0.52 1.714 1.185 0.48 -0.99 1.786 0.979 1.264 1.296 -0.90 2.010 0.52 0.41 0.59 1.201 -0.76
$\mathrm{TS\text{-}I5}_2$
-5.4
-4.8
1.773 1.830 0.51 1.557 0.53 -0.98 1.761 -1.03 0.51 1.738 1.859 -0.99 1.957 0.45 -0.81 0.64 0.49 -0.73 0.42 1.241 1.215
5b
$\mathrm{I5}_3$
1.483 1.470 -0.99 1.534 0.53 0.52 -0.99 0.52 1.614 1.611 1.702 -0.75 -0.99 0.55 -0.95 1.746 0.52 0.41 1.279 1.196
5ab
4.5
6.5
1.694 1.347 -0.98 1.724 1.206 0.51 -0.99 0.53 1.205 0.51 1.762 1.833 0.58 -0.77 0.50 -0.91 1.417 -0.97 1.267 1.201
$\mathrm{TS\text{-}I5}_3$
-7.0
-7.3
1.840 1.637 -1.01 1.843 -0.98 -0.97 0.51 1.628 0.51 0.52 1.927 0.64 -0.75 1.997 -0.81 0.45 1.606 0.42 1.242 1.215
5b'

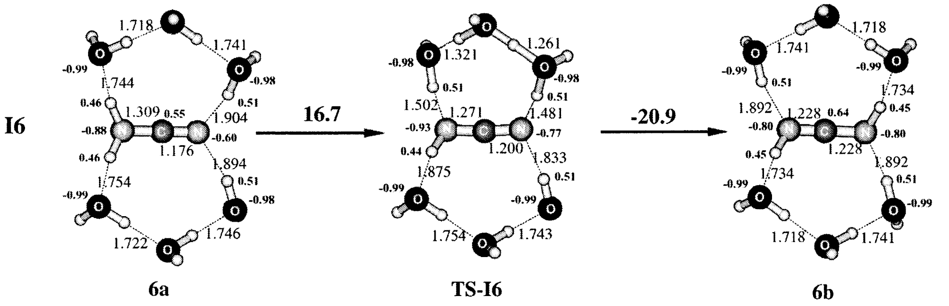

Figure 2. Best molecular geometries for reactants, TSs, and products of the cyanamide → carbodiimide isomerization in the absence or in the presence of $(H_2O)_n$ clusters (n = 1, ..., 6). Distances are in angstroms (large characters), and atomic charges are printed in boldface (small characters). The energy values reported above the arrows (boldface) are ΔG values (in kcal mol^{-1}) computed at the PCM-B3LYP/6-31G(d,p) level of theory. Below arrows are the corresponding PCM-MP2/6-31G(d,p) values (italic). The values associated with the left arrows are activation free energies $\Delta G^{\#} = G(\mathbf{TS-In}) - G(\mathbf{na})$. The ΔE values (in kcal mol^{-1}) without PCM correction, for the **na** → **TS−In** and **TS−In** → **nb**, computed at B3LYP/6-31G(d,p) level are (**I1**) 36.4, −34.1; (**I2**) 21.3, −16.8; (**I3**) 17.8, −13.5; (**I4**) 15.0, −10.0; (**I5$_1$**) 8.4, −1.0; (**I5$_2$**) 3.4, −6.7; (**I5$_3$**) 5.0, −6.3; (**I6**) 18.9, −14.2. The corresponding ΔE values computed at MP2/6-31G(d,p) level are (**I1**) 42.4, −33.4; (**I2**) 27.7, −17.6; (**I3**) 24.3, −14.8; (**I4**) - - -, - - -; (**I5$_1$**) 13.3, −0.4; (**I5$_2$**) 0.4, −4.1; (**I5$_3$**) 5.0, −7.3; (**I6**) - - -, - - -.

TABLE 1: Structural Parameters of Cyanamide Calculated at Different Levels of Theory[a]

	N≡C	C−N	N−H	N≡C−N	C−N−H
B3LYP/6-31G(d,p)	1.166	1.346	1.103	177.4	114.9
B3LYP/6-311++G(d,p)	1.158	1.340	1.011	177.4	115.9
B3LYP/6-31G(3df,2p)	1.154	1.134	1.010	177.2	115.2
B97/6-31G(d,p)	1.169	1.349	1.014	177.4	114.9
MP2/6-31G(d,p)	1.183	1.356	1.010	176.9	113.1
CCSD/6-31G(d,p)	1.170	1.360	1.360	177.2	113.1
MP2/cc-pVDZ	1.187	1.366	1.020	176.4	111.0
MP2/cc-pVTZ	1.172	1.351	1.008	176.7	112.9
MP2/cc-pVQZ	1.169	1.347	1.007	176.8	113.4
exp.[b]	1.165	1.350	1.008	174.8	113.0

[a] Bond lengths (Å), angles (degree). [b] From ref 12.

TABLE 2: Structural Parameters of Carbodiimide Calculated at Different Levels of theory[a]

	N=C	N−H	N−C−N	C=N−H	H−N··N−H
B3LYP/6-31G(d,p)	1.228	1.015	170.6	118.6	93.7
B3LYP/6-311++G(d,p)	1.221	1.012	170.8	120.0	93.5
B3LYP/6-31G(3df,2p)	1.218	1.011	170.7	119.7	93.1
B97/6-31G(d,p)	1.231	1.015	170.2	118.1	93.7
MP2/6-31G(d,p)	1.236	1.011	169.2	118.4	93.8
MP2/cc-pVDZ	1.242	1.022	169.7	115.7	93.0
MP2/cc-pVTZ	1.228	1.010	170.1	118.2	92.9
MP2/cc-pVQZ	1.225	1.008	170.0	119.0	93.0
CCSD/6-31G(d,p)	1.233	1.102	170.5	116.8	93.6
CCSD(T)/cc-pVDZ[b]	1.245	1.025	170.2	114.3	89.4
CCSD(T)/cc-pVTZ[b]	1.230	1.012	170.6	116.7	89.2
CCSD(T)/cc-pVQZ[b]	1.226	1.010	170.5	117.5	89.2
exp.[c]	1.224	1.007	170.6	118.6	89.0

[a] Bond lengths (Å), angles (degree). [b] From ref 11. [c] From ref 10.

is mediated by the water molecule. The role of H_2O in lowering the activation energy is confirmed in path **I2** (Figure 2), where $\Delta G^{\#}$ = 19.6 kcal mol^{-1}. The TS corresponds to an eight-membered ring with a relatively small structural rearrangement with respect to reactants and products; at TS the N−C−N angle is 167.6°, only 4.1° smaller than in **2b**. Interestingly, significant changes of the atomic charges on the nitrogen atoms occur in adducts **2a** and **2b**, caused by the presence of water molecules, which are able to smooth the electronic rearrangement along the reaction path (see Table 4).

The inclusion of a third water molecule gives rise to energy changes significantly smaller than in the previous cases. The $\Delta G^{\#}$ value of **I3** (see Figure 2) is only 2.9 kcal mol^{-1} lower than that of **I2**. The water adducts **3a** and **3b**, as well as **TS−I3**, are involved in an extended network of H-bonds. At **TS−I3**, the N−C−N angle is equal to 170°, very close to that computed for free carbodiimide. The three water molecules contribute to a further reduction of the electronic charge rearrangement (see Table 4).

TABLE 3: DFT Energies (in kcal·Mol^{-1}) of the Cyanamide → Carbodiimide Isomerization (ΔE) Computed with Different Exhange-correlation Fucntionals[a]

	ΔE		ΔE
HCTH	−2.2	B3P86	0.0
SVWN5	−3.7	B3PW91	0.1
Xalpha	−3.8	B97	0.5
BLYP	−1.5	B3LYP	0.5
PW91	−2.2	B3LYP/6-311++G(d,p)	0.5
MPW1PW91	0.6	B3LYP/6-311G(3df,2p)	−0.5
BHandHLYP	−3.5		

[a] The functionals used are defined as follows: HTCH is the exchange-correlation functional of Handy[28] as implemented in Cadpac;[29] SVWN5 is the Slater exchange[30] with the Vosko-Wilk-Nusair correlation functional V;[31] Xalpha is pure Slater exhange;[30] BLYP is the gradient corrected exchange of Becke[20a] with the LYP correlation functional;[32] PW91 is the Perdew and Wang exchange-correlation functional;[33] MPW1PW91 is the one parameter form of PW91 functional as modified by Barone and Adamo;[34] BHandHLYP is the functional with half of Hartree−Fock exchange and LYP non local correlation functional as implemented in Gaussian98;[26] B3P86 is the Becke three paramenter functional with the non local correlation provided by the Perdew 86 functional;[35] B3PW91 is the Becke three paramenter functional with the non local correlation provided by the Perdew 91 functional; B97 is the exchange-correlation functional of Becke.[36] If not otherwise indicated, the adopted basis set is 6-31G(d,p).

The system including four water molecules (**4a**, **4b**, **TS−I4**, path **I4** of Figure 2) is characterized by an activation free energy equal to 14.2 kcal mol^{-1}, 2.5 kcal mol^{-1} lower than that of **I3**.

The hydrated complexes **5a** and **5b** are probably characterized by the existence of several local minima, differing in the arrangement of H-bond network. To obtain a reasonable description of the lowest energy forms of **5a** and **5b**, several optimizations have been carried out starting from different initial conditions. Even if such a procedure cannot necessarily give the global minimum, the results of Figure 2 are fairly reliable. For the isomerization reaction, we were able to identify a (weakly) stable intermediate **5ab**, which opens the possibility of the following different pathways **5a** → **TS−I5$_1$** → **5ab**, **5ab** → **TS−I5$_2$** → **5b**, and **5ab** → **TS−I5$_3$** → **5b′**. This indicates that **5ab** can be converted into **5b** in two different ways. In particular, in the path **I5$_1$** ($\Delta G^{\#}$ = 8.6 kcal mol^{-1}), the proton transfer from N^{D} to N^{A} occurs via the ionic $(H_2O)_4H_3O^+$-HNCN− intermediate **5ab** (see Figure 2) lying only 1.5 kcal

SCHEME 1: Atom Labels Used in the Text for the Isomerization (a), Cyanamide Hydrolysis (b), and Carbodimide Hydrolysis (c)[a]

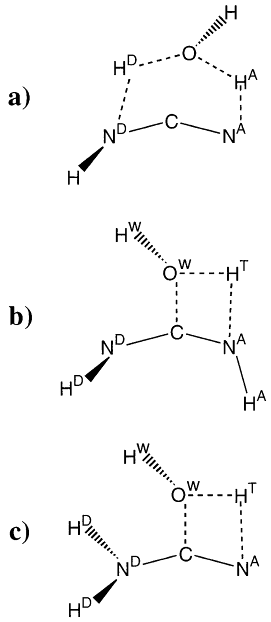

[a] Hydrogen donor and acceptor N atoms are labelled D and A, respectively. Hydrogen atom undergoing transfer from N^D to N^A is denoted as H^T; H^W and O^W are atoms belonging to water molecules

TABLE 4: Change in Natural Atomic Charges during Cyanamide → Carbodiimide Isomerization

	N^D	H^D	N^A	H^A	C
a → TS−I	0.22	0.07	0.01	0.07	−0.29
TS−I →b	0.00	−0.10	−0.39	−0.10	0.49
1a → TS−I1	−0.02	0.08	−0.22	0.02	0.09
TS−I1 → 1b	0.18	−0.04	−0.11	−0.09	0.12
2a → TS−I2	−0.04	0.06	−0.20	0.00	0.07
TS−I2 → 2b	0.14	−0.01	−0.05	−0.07	0.09
3a → TS−I3	−0.05	0.05	−0.16	0.00	0.05
TS−I3 → 3b	0.12	0.00	−0.02	−0.07	0.08
4a → Ts-I4	−0.01	0.05	−0.25	0.00	0.06
TS−I4 → 4b	0.07	−0.01	0.09	−0.07	0.07
5a → TS−I5$_1$	−0.04	0.04	−0.13	0.00	0.02
TS−I5$_1$ → 5ab	0.00	0.01	−0.06	0.00	0.01
5ab → TS−I5$_2$	0.05	0.00	−0.01	−0.04	0.04
TS−I5$_2$→ 5b	0.09	−0.01	0.03	−0.03	0.05
5ab → TS−I5$_3$	0.04	−0.01	−0.02	−0.02	0.03
TS−I5$_3$ → 5b′	0.10	0.00	0.02	−0.05	0.06
6a → TS−I6	−0.05	0.05	−0.17	0.00	0.03
TS−I6 → 6b	0.13	0.00	−0.03	−0.06	0.06

mol^{-1} lower in energy than **TS−I5$_1$**. In the path **I5$_2$** ($\Delta G^\# = 2.4$ kcal mol^{-1}), the conversion **5ab** → **5b** takes place via a concerted transfer of two protons, and, finally, in **I5$_3$** ($\Delta G^\# = 4.5$ kcal mol^{-1}), via the transfer of three protons leading to the slightly different form **5b′**.

The reaction path **I6**, including **6a** and **6b** (see Figure 2), is characterized by an activation free energy very similar to that computed with fewer water molecules, indicating that the sixth water molecule does not really take part in the isomerization, or in other words, that the energy data are converged with respect to the number of water molecules.

It is important to observe that the hydration energy of cyanamide is always larger than that of carbodiimide. The PCM-B3LYP/6-31G(d,p) value of $\Delta G_{\mathbf{a-b}}$ is 1.9 kcal mol^{-1} for both **a** → **b** and **1a** → **1b** mechanisms, 4.9 and 3.8 kcal mol^{-1} when the isomers are solvated with two and three water molecules, respectively. These values remain almost constant upon addition of more water molecules.

Mechanism of Hydrolysis of Cyanamide and Carbodiimide. The hydrolysis of **a** and **b** (see eqs 2 and 3 of the Introduction) have been studied in the presence of up to four explicit water molecules by DFT and MP2 calculations, in vacuo and including PCM corrections. In the following, only ΔG values from PCM treatment will be discussed. ΔE values from in vacuo calculations are reported in the captions of Figures 3 and 4 for the hydrolysis of **a** and **b**, respectively.

Hydrolysis of Cyanamide. The reaction PCM ΔG values are reported in Figure 3 for the **na** → **TS-An** ($\Delta G^\#$ value) and **TS-An** → **nc** steps. For the **na** → **nc** reaction ($n = 1, 2$; path **A1** and **A2** of Figure 3), our PCM-B3LYP estimates of $\Delta G^\#$ are considerably high: 50.7 and 31.7 kcal mol^{-1}, respectively. Three water molecules may originate three different pathways **A3$_1$**, **A3$_2$**, and **A3$_3$** (Figure 3). In **A3$_1$**, the third water molecule is involved in the proton transfer leading to a TS characterized by a sort of eight-membered ring and a $\Delta G^\#$ slightly higher than in **A2**. The reaction path **A3$_2$** has the third water molecule near to the nonreacting nitrogen atom but not involved in the proton transfer and a value of $\Delta G^\# = 29.8$ kcal mol^{-1} slightly lower than in **A2**. In the third pathway **A3$_3$**, two water molecules are directly involved in the proton transfer forming a six-membered ring at TS, but also in this case, the activation energy does not decrease with respect to **A2**. Therefore, we observe that, in the most favorable case, the third water molecule leads to a stabilization of the TS of only 1.9 kcal mol^{-1} with respect to **A2**.

The system with four water molecules is characterized by a high number of degrees of freedom and cannot be fully investigated. Our choice to put the fourth water molecule near to the nonreactive N atom leads to several reaction pathways not commented on here for brevity. The best mechanism seems to be the path **A4** of Figure 3, characterized by $\Delta G^\# = 31.1$ kcal mol^{-1}, about 1 kcal mol^{-1} higher than the value of **A3$_2$**.

Stereochemistry constraints of water addition to cyanamide can produce only the less stable *Z* configuration of the $C{=}N^A$ bond. Considering the products with the most stable arrangement of the water molecules (not shown in Figure 3), the $\Delta G_{\mathbf{na \to nc}}$ for the hydrolysis of cyanamide is found to be equal to −18.5, −19.9, −15.3, and −19.9 kcal·mol^{-1} for $n = 1, ..., 4$, respectively.[37]

Hydrolysis of Carbodiimide. The reaction **1b** → **1c** (path **B1** of Figure 4) leads to **TS−B1**, which is a sort of a strained four-membered ring, characterized by a high $\Delta G^\#$ (42.8 kcal·mol^{-1}). The activation free energy decreases to 24.6 kcal mol^{-1} in **2b** → **2c** (path **B2** of Figure 4).

Our DFT results for the reaction **3b** → **3c** can be compared with the MP2 results of Glaser et al.[14] We confirm that the reaction **b** + 3H$_2$O → **c** + 2H$_2$O can follow two different reaction paths (**B3$_1$** and **B3$_2$** of Figure 4). In the first path, the third water molecule takes part in the proton transfer leading to an eight-membered ring TS without, however, a significant change of the activation energy with respect to **B2**. In the second path **B3$_2$**, the third water molecule is located near the nonreacting nitrogen atom and plays a direct role in the proton transfer. **TS−B3$_2$** is similar to **TS−B2**, but with an activation energy lower by about 7 kcal mol^{-1}. Glaser et al.[14] suggested that the role of the third water molecule is to enhance the charge delocalization, a view fully confirmed by our data on charge reorganizations reported in Table 5.

Also, the **4b** → **4c** reaction can be characterized by several arrangements of the water molecules. We have identified two

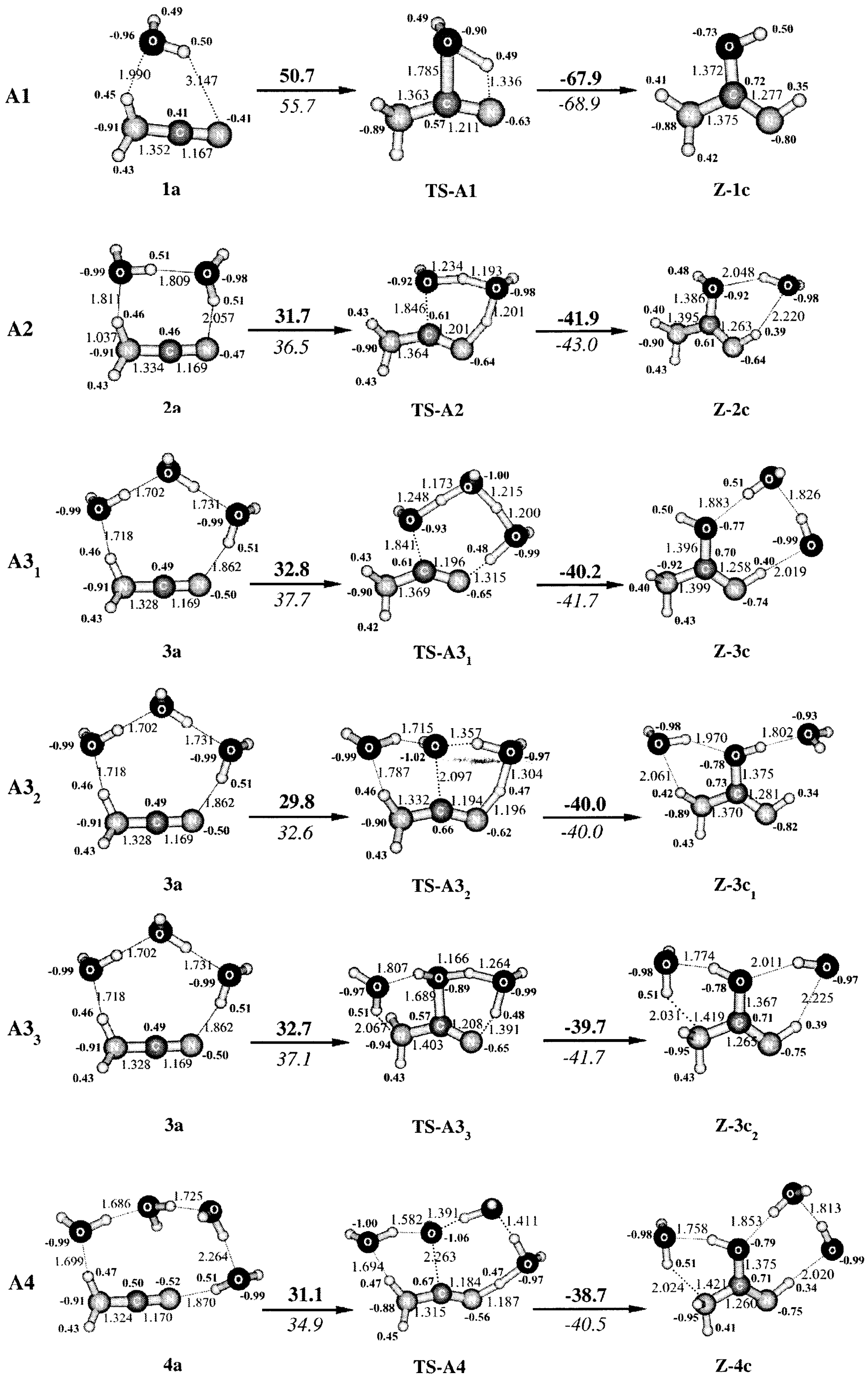

Figure 3. Best molecular geometries for reactants, TSs, and products of the hydrolysis of cyanamide mediated by $(H_2O)_n$ clusters (n = 1, ..., 4). See the caption of Figure 2. The ΔE values (in kcal mol^{-1}) without PCM corrections, for the **na** → **TS-An** and **TS-An** → **nc**, are (**A1**) 52.8, −65.9; (**A2**) 34.9, −38.9; (**A3$_1$**) 35.2, −46.5; (**A3$_2$**) 36.1, −39.1; (**A3$_3$**) 38.6, −40.8; (**A4**) 31.9, −33.7. The corresponding ΔE values computed at MP2/6-31G(d,p) level are (**A1**) 59.7, −66.5; (**A2**) 42.2, −40.4; (**A3$_1$**) 42.5, −47.8; (**A3$_2$**) 42.9, −41.2; (**A3$_3$**) 44.2, −42.0; (**A4**) 39.2, −36.7.

most probable situations: the first (**B4$_1$**) is related to **TS−B3$_1$** with the fourth water molecule placed near to the nonreactive nitrogen atom: the proton transfer takes place via a six-membered ring TS characterized by a $\Delta G^{\#}$ of 12.4 kcal mol^{-1}, about 5 kcal mol^{-1} lower than in **B3$_2$**. The second path **B4$_2$** is similar to **B4$_1$** but the $C{=}N^D$ bond has the *Z* configuration at **TS−B4$_2$** (see Figure 4). The proton transfer is promoted by two water molecules, but the computed activation energy is significantly higher than that of **B4$_1$**.

The results on energetics of the hydrolysis reaction of carbodiimide may be summarized as follows: the reaction energies depend on different shapes and extents of the hydrogen bond networks between reagents and products as well as on the existence of *E* or *Z* configuration of the $C{=}N^D$ bond in the product. The reaction product with imine group in *E* is always more stable than in *Z* configuration by a few kcal mol^{-1}. The reaction energies computed by considering the most stable arrangement of the products for the reactions with n = 1, ..., 4 are equal to −20.4, −19.2, −18.7, and −23.3 kcal mol^{-1}, respectively.

Discussion

The results of our systematic investigation allow us to draw some general conclusions. From a methodological point of view,

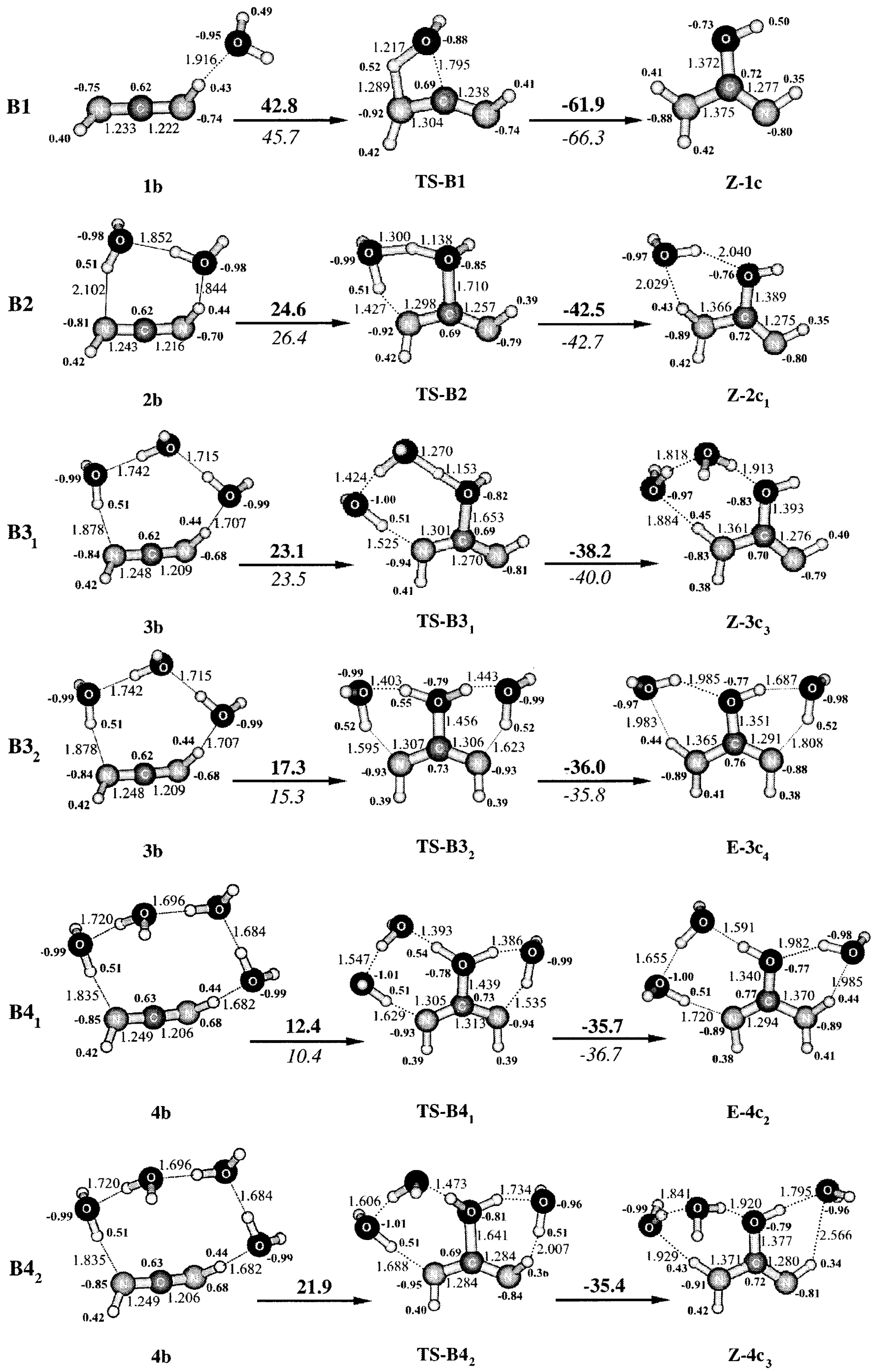

Figure 4. Best molecular geometries for reactants, TSs, and products of the hydrolysis of carboddimide mediated by $(H_2O)_n$ clusters ($n = 1, ..., 4$). See the caption of Figure 2. The ΔE values (in kcal mol^{-1}) without PCM correction, for the **nb** → **TS−Bn** and **TS−Bn** → **nc**, are (**B1**) 40.2, −56.6; (**B2**) 27.9, −39.8; (**B3$_1$**) 28.4, −37.0; (**B3$_2$**) 18.0, −35.2; (**B4$_1$**) 12.5, −33.8; (**B4$_2$**) 29.1, −37.6. The corresponding ΔE values computed at MP2/6-31G(d,p) level are (**B1**) 43.7, −59.5; (**B2**) 32.1, −43.3; (**B3$_1$**) 33.2, −42.0; (**B3$_2$**) 22.9, −39.3; (**B4$_1$**) 19.7, −39.3; (**B4$_2$**) - - -, - - -.

we note that the B3LYP activation energies are systematically lower than the corresponding MP2 values and probably underestimated. This confirms the finding of Lynch and Truhlar[27] that B3LYP slightly underestimates the energy barriers in proton-transfer reactions.

As for the reactions **na** → **nc** and **nb** → **nc**, our DFT results are converged in terms of number of water molecules explicitly considered, and indicate an activation energy for **a** significantly higher than for **b**. Such a difference is due to a different electrophilic character of the carbon atom in the two isomers. In fact, the net charge on the C atom is higher in **b** (0.65) than in **a** (0.45). Therefore, carbodiimide is an electrophyle stronger than cyanamide, a characteristic conserved also in water adducts.

Glaser et al.[14] proved that in the hydrolysis of carbodiimide mediated by three water molecules the activation process is accompanied by an increased positive charge of the O^WH^W group (labels of atoms defined in Schemes 2a and 3a) and an increased negative charge of the N^DH^D group, with an enhanced tendency to form H bonds. As shown in Table 5, such variations of the atomic charges predicted by MP2 calculations[14] are qualitatively reproduced also by our B3LYP calculations. Furthermore, Glaser et al.[14] suggested that also the structure of

TABLE 5: Change in Natural Atomic Charges during Carbodiimide and Cyanamide Hydrolysis

	H^W	O^W	NH^D	NH^A	H^T	C
			Cyanamide			
1a→TS-A1	−0.01	0.06	0.01	−0.22	−0.01	0.16
2a→TS-A2	0.00	0.07	−0.02	−0.17	−0.04	0.14
3a→TS-A3$_1$	0.49	0.07	−0.03	−0.15	−0.03	0.12
3a→TS-A3$_2$	−0.08	−0.02	0.02	−0.12	−0.00	0.16
3a→TS-A3$_3$	0.04	0.12	0.15	0.15	−0.03	0.08
4a→TS-A4	−0.03	−0.06	0.03	−0.08	−0.04	0.17
			Carbodiimide			
1b→TS−B1	0.00	0.05	−0.02	−0.15	0.03	0.07
2b→TS−B2	0.00	0.13	−0.14	−0.11	0.00	0.07
3b→TS−B3$_1$	0.03	0.17	−0.21	−0.10	−0.01	0.07
3b→TS−B3$_2$	0.06	0.21	−0.30	−0.12	0.00	0.11
4b→TS−B4$_1$	0.06	0.22	−0.31	−0.11	0.00	0.10
4b→ TS−B4$_2$	0.05	0.19	−0.24	−0.12	−0.01	0.06

the TS may be affected by the presence of the nonreactive water molecule. In fact, when the geometries of **TS−B2** and **TS−B3$_2$** are compared, one can note an enhanced interaction between C and O^W atoms (the $C-O^W$ bond length in **TS−B3$_2$** is 0.254 Å shorter than that in **TS−B2**) and a parallel reduced strength of the H^T-N^A bond (the H^T-N^A distance in **TS−B3$_2$** is 0.168 Å longer than in **TS−B2**).

Our results underline that electronic rearrangements occurring in the hydrolysis of cyanamide are significantly different from those of carbodiimide. As shown in Table 5, for the pathways **A1**, **A2**, and **A3**, concerning **na** → **nc** reactions in which all of the water molecules are involved in the proton transfer, the O^WH^W group is more positively charged at TS, whereas the N^DH^D group is more negatively charged. The trend is the same also for the **nb** → **nc** systems, but the variations of charges in this case are significantly larger. It is noteworthy that the geometries of the transition states **TS-A3$_2$** and **TS-A4** are strongly affected by the presence of the water molecule with no reactive character in carbodiimide (see Figure 4). In the reaction path **A3$_3$**, the nonreactive water molecule is placed in a position equivalent to that in the **B3$_2$** and **B4$_1$** pathways. Therefore, charge dispersion similar to that discussed for these reaction paths should be expected. In fact, the variation of the atomic charges going from the reactant to the TS (see Table 5) are similar to those discussed in the hydrolysis of carbodiimide. The nonreactive water molecule has important effects on the geometry of the **TS-A3$_3$**, similar to those observed in the **B3$_2$** and **B4$_1$** mechanisms, but little effect on the stabilization of the TS.

In summary, our results show that the most relevant electronic mechanism responsible for the decrease of the activation energy in the hydrolysis reaction is the charge reorganization induced by water molecules. The difference in the electrophilic character of the carbon atom in the two tautomers, as well as the inability of a nonreactive water molecule to induce charge relaxation in the hydrolysis of cyanamide are synergic effects, which determine the large difference of the activation energy in the hydrolysis of cyanamide and carbodiimide.

Finally, when $\Delta E^{\#}$ values in vacuo are compared with the $\Delta G^{\#}$ ones of the PCM treatment, one can easily observe that the effect associated with the bulk solvent is relatively small, probably because the main solvent contribution are already taken into account by the explicit water molecules.

In the case of **1a** → **1b** and **2a** → **2b** reactions, all of the ΔE (and $\Delta E^{\#}$) values have been corrected for BSSE.[23] The error due to the incompleteness of the basis is within the range 3−6 kcal mol^{-1} but is roughly constant for **na**, **TS**, and **nb** species of the same reaction path. Therefore, $\Delta E^{\#}$ and reaction energies remain unchanged.

SCHEME 2: Energy Profiles of the "direct" and "two-step" Reaction Paths for the Hydrolysis of Cyanamide

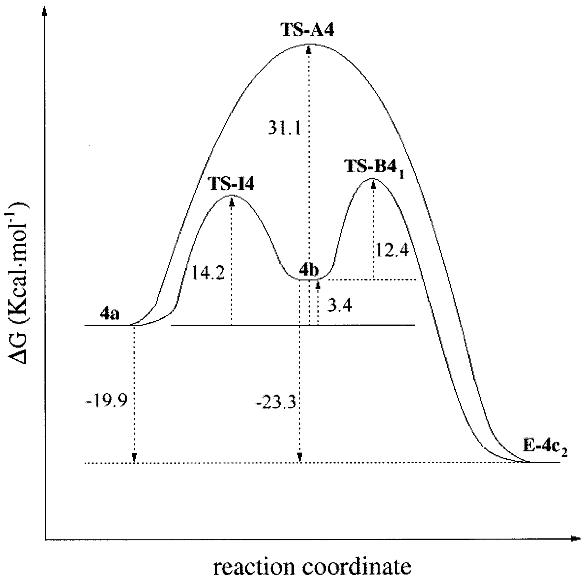

The conclusion can be drawn that the hydrolysis of cyanamide is kinetically unfavorable because of the large energy barrier. However, cyanamide can be easily converted into carbodiimide through a tautomerization reaction strongly favored by the presence of water molecules. Carbodiimide is thermodinamically less stable than cyanamide by about 4 kcal mol^{-1} and therefore is expected to be present in a very small amount at thermal equilibrium. However, the hydrolysis of carbodiimide leading to isourea is both thermodinamically and kinetically favorable so that carbodiimide can be considered a suitable stable intermediate in hydrolysis of cyanamide. The energetics of such a "two step" mechanism is graphically shown in Scheme 2 and compared with the mechanism of "direct hydrolysis" of cyanamide.

Conclusions

The accurate theoretical study of the chemistry of **a** and **b** tautomers in the gas phase predicts that cyanamide is 2.5 kcal mol^{-1} more stable than carbodiimide. DFT-B3LYP calculations show that the activation energy for the isomerization reaction **a** → **b**, extremely high in the gas phase, is drastically reduced by cooperative effects of a few water molecules.

The direct hydrolysis of cyanamide is a difficult process, even in the presence of water, because of its considerably high activation energy, but a much easier process for carbodiimide. The difference between the activation energy for the hydrolysis of the two tautomers can be explained by the different electrophilic character of the C atom and a less efficient charge redistribution in the case of cyanamide hydrolysis. This suggests that the most probable path for hydrolysis of cyanamide involves first the formation of carbodiimide and then its subsequent hydrolysis.

Supporting Information Available: Cartesian coordinates of the optimized geometries of the products labeled E−1c, E−2c, E−3c1, and E−4c1. This material is available free of charge via the Internet at http://pubs.acs.org.

References and Notes

(1) Forgione P. in *Ullman's Encyclopedia of Industrial Chemistry*; VCH: Weiheim, Germany, 1987; Vol. A8, p 139.

(2) (a) Steinman, G.; Lemmon, R. M.; Calvin, M. *Proc. Natl. Acad. Sci.* **1964**, *2*, 27. (b) Schimpl, A.; Lemmon, R. M.; Calvin M. *Science* **1965**, *147*, 49.

(3) (a) Khorana, H. G. *Chem. Rev.* **1953**, *53*, 145. (b) Kurzer, F.; Douraghi-Zadeh, K. *Chem. Rev.* **1967**, *67*, 107. (c) Williams, A.; Ibrahim, I. T. *Chem. Rev.* **1981**, *81*, 589.

(4) (a) *The Carbonic Anhydrase*; Dogson, S. J., Tashian, R. E., Gross C., Carter, N. D., Eds.; Plenium Press: New York, 1991. (b) Supuran C. T. In *Carbonic Anhydrase and Modulation of Physiologic and Pathologic Processes in the Organism*; Puscas, I., Eds.; Helicon: Timisoara, Romania, 1994; pp 29−111. (c) Christianson, D. W.; Fierke, C. A. *Acc. Chem. Res.* **1996**, *29*, 331. (d) Christianson, D. W.; Ippolito, J. A. In *Carbonic Anhydrase*; Botrè, F., Gros, G., Storey, B. T., Eds.; VCH: New York, 1991; pp 95−110. (d) Hewett-Emmett, D.; Tashian, R. E. *Mol. Phylogenet. Evol.* **1996**, *5*, 50. (e) Lindskog, S.; Liljas, A. *Curr. Opin. Struct. Biol.* **1993**, *3*, 15. (f) Lindskog, S.; Liljas, A. *Roum. Chem. Q. Rev.* **1994**, *2*, 243. (g) Maren, T. H. *Physiol. Rev.* **1967**, *47*, 595.

(5) (a) Liljas, A.; Håkansson, K.; Jonsson, B. H.; Xue, Y. *Eur. J. Biochem*. **1994**, *219*, 1. (b) Silverman, D. N.; Lindskog, S. *Acc. Chem. Res*. **1988**, *21*, 30. (c) Baird, T. T.; Waheed, A.; Okuyama, T.; Sly, W. S.; Fierke, C. A. *Biochemistry* **1997**, *36*, 2669. (d) Simonsson, I.; Jonsson, B. H.; Lindskog, S. *Biochem. Biophys. Res. Commun*. **1982**, *108*, 1406. (e) Briganti, F.; Piettarelli, R.; Scozzafava, A.; Supuran, C. T. *Eur. J. Med. Chem*. **1996**, *31*, 1001. (f) Bertini, I.; Luchinat, C. *Acc. Chem. Res*. **1983**, *16*, 272. (g) Bertini, I.; Luchinat, C.; Scozzafava, A. *Struct. Bonding* **1982**, *48*, 45. (h) Bertini, I.; Luchinat, C.; Mangani, S.; Pieratelli, R. *Comments Inorg. Chem*. **1995**, *17*, 1. (i) Briganti, F.; Mangani, S.; Scozzafava, A.; Vernaglione, G.; Supuran, C. T. *Biochemistry* **1997**, *36*, 10384. (j) Eriksson, A. E.; Kylsten, P. M.; Jones, T. A.; Liljas, A. *Proteins Struct. Func. Genet*. **1988**, *4*, 283. (k) Mangani, S.; Hakansson, K. *Eur. J. Biochem*. **1992**, *210*, 867. (l) Kumar, V.; Kannan, K. K. *J. Mol. Biol*. **1994**, *241*, 226. (m) Mangani, S.; Liljas, A. *J. Mol. Biol*. **1993**, *232*, 9. (n) Nair, S. K.; Ludwig, P. A.; Christianson, D. W. *J. Am. Chem. Soc*. **1994**, *116*, 3659. (o) Smith, G. M.; Alexander, R. S.; Christianson, D. W.; McKeever, B. M.; Ponticello, G. S.; Springer, J. P.; Randall, W. C.; Baldwin, J. J.; Habecker, C. N. *Protein Sci*. **1994**, *3*, 118.

(6) Briganti, F.; Mangani, S.; Scozzafava, A.; Vernaglione, G.; Supuran, C. T. *J. Biol. Inorg. Chem*. **1999**, *4*, 528.

(7) Guerri, A.; Briganti, F.; Scozzafava, A.; Supuran, C. T.; Mangani, S. *Biochemistry* **2000**, *39*, 12391.

(8) (a) Baughen, A. E. *Can. Chem. Proc. Ind.* **1944**, *28*, 805. (b) Bann, B.; Miller, S. A. *Chem. Rev.* **1958**, *58*, 131. (c) Hill, S. V.; Williams, A.; Longridge, J. L. *J. Chem. Soc., Perkin Trans. 2* **1984**, 1009. (d) von Michaud, H.; Goll, W.; Hammer, B.; von Seyerl, J.; Sturm, W.; Weiss, S.; Yungman, R. *Chemiker-zeitung* **1988**, *10*, 287. (e) Pankratov, V. A.; Chesnokova, A. Z. *Russ. Chem. Rev.* **1989**, *58*, 879.

(9) Kawauchi, S.; Tachibana, A.; Mori, M.; Shibusa, Y.; Yamabe, T. *J. Mol. Struct. (TEOCHEM)* **1994**, *310*, 255.

(10) (a) Birk, M.; Winnewisser, M.; Cohen, E. *J. Mol. Spectrosc.* **1989**, *136*, 402. (b) Jabs, W.; Winnewisser, M.; Belov, S. P.; Lewen, F.; Maiwald, F.; Winnewisser, G. *Mol. Phys.* **1999**, *97* (1−2), 213.

(11) Koput, J.; Jabs, W.; Winnewisser, M. *Chem. Phys. Lett.* **1998**, *295*, 462.

(12) Torrie, B. H.; Vondreele, R.; Larson, A. C. *Mol. Phys.* **1992**, *76*, 405.

(13) Nguyen, M. T.; Raspoet, G.; Vanquickenborne, L. G. *J. Chem. Soc., Perkin Trans.* **1999**, *2*, 813.

(14) Lewis, M.; Glaser, R. *J. Am. Chem. Soc.* **1998**, *120*, 8541.

(15) Møller, C.; Plesset, M. S. *Phys. Rev.* **1934**, *46*, 618.

(16) Pople, J. A.; Krishnan, R.; Schlegel, H. B.; Binkey, J. S. Theoretical Models Incorporating Electron Correlation. *Int. J. Quantum Chem. Symp.* **1976**, *10*, 1.

(17) Parr, R. G.; Yang, W. In *Density Functional Theory of Atoms and Molecules*; Oxford University Press: New York, 1989.

(18) Hariharan, P. C.; Pople, J. A. *Mol. Phys.* **1974**, *27*, 209.

(19) Dunning, T. H., Jr. *J. Chem. Phys.* **1990**, *92*, 551. (b) Wilson, A. K.; van Mourik, T.; Dunning, T. H., Jr. *J. Mol. Struct.* **1996**, *388*, 339.

(20) (a) Becke, A. D. *Phys. Rev. A* **1988**, *38*, 3098. (b) Becke, A. D. *J. Chem. Phys.* **1992**, *96*, 2155. (c) Becke, A. D. *J. Chem. Phys.* **1993**, *98*, 5648. (d) Stevens, P. J.; Devlin, F. J.; Chablowski, C. F.; Frisch, M. J. *J. Phys. Chem.* **1994**, *98*, 11623.

(21) (a) Peng, C.; Schlegel, H. B. *Isr. J. Chem.* **1994**, *33*, 449. (b) Peng, C.; Ayala, P. J.; Schlegel, H. B.; Frisch, M. J. *J. Comput. Chem.* **1996**, *17*, 49.

(22) (a) Miertus, S.; Scrocco, E.; Tomasi, J. *Chem. Phys.* **1981**, *55*, 117. (b) Miertus, S.; Tomasi, J. *Chem. Phys.* **1982**, *65*, 239. (c) Cossi, M.; Barone, V.; Cammi, R.; Tomasi, J. *Chem. Phys. Lett.* **1996**, *255*, 327.

(23) van Duijneveldt, F. B.; van Duijneveldt-van de Rijdt, J. G. C. M.; van Lenthe, J. H. *Chem. Rev.* **1994**, *94*, 1873.

(24) (a) Reed, A. E.; Weinstock, R. B.; Weinhold, F. *J. Chem. Phys.* **1985**, *83*, 735. (b) Reed, A. E.; Curtiss, L. A.; Weinhold, F. *Chem. Rev.* **1988**, *88*, 899. (c) Foster, J. P.; Weinhold, F. *J. Am. Chem. Soc.* **1980**, *102*, 7211. (d) Brunck, T. K.; Weinhold, F. *J. Am. Chem. Soc.* **1978**, *101*, 1700. (e) Reed, A. E.; Weinhold, F. *J. Chem. Phys.* **1985**, *83*, 1736. (f) Weinhold, F.; Carpenter, J. E. In *The Structure of Small Molecules and Ions*, Plenum: New York, 1988; p 227.

(25) (a) Curtiss, L. A.; Jones, C.; Trucks, G. W.; Raghavachari, K.; Pople, J. A. *J. Chem. Phys.* **1990**, *93*, 2537. (b) Curtiss, L. A.; Jones, C.; Raghavachari, K.; Pople, J. A. *J. Chem. Phys.* **1991**, *94*, 7221.

(26) Frisch, M. J.; Trucks, G. W.; Schlegel, H. B.; Scuseria, G. E.; Robb, M. A.; Cheeseman, J. R.; Zakrzewski, V. G.; Montgomery, J. A., Jr.; Stratmann, R. E.; Burant, J. C.; Dapprich, S.; Millam, J. M.; Daniels, A. D.; Kudin, K. N.; Strain, M. C.; Farkas, O.; Tomasi, J.; Barone, V.; Cossi, M.; Cammi, R.; Mennucci, B.; Pomelli, C.; Adamo, C.; Clifford, S.; Ochterski, J.; Petersson, G. A.; Ayala, P. Y.; Cui, Q.; Morokuma, K.; Malick, D. K.; Rabuck, A. D.; Raghavachari, K.; Foresman, J. B.; Cioslowski, J.; Ortiz, J. V.; Stefanov, B. B.; Liu, G.; Liashenko, A.; Piskorz, P.; Komaromi, I.; Gomperts, R.; Martin, R. L.; Fox, D. J.; Keith, T.; Al-Laham, M. A.; Peng, C. Y.; Nanayakkara, A.; Gonzalez, C.; Challacombe, M.; Gill, P. M. W.; Johnson, B. G.; Chen, W.; Wong, M. W.; Andres, J. L.; Head-Gordon, M.; Replogle, E. S.; Pople, J. A. *Gaussian 98*, revision A.7; Gaussian, Inc.: Pittsburgh, PA, 1998.

(27) Lynch, B. J.; Truhlar, D. G. *J. Chem. Phys. A* **2001**, *105*, 2936.

(28) Hamprecht, F. A.; Cohen, A. J.; Tozer, D. J.; Handy, N. C. *J. Chem. Phys.* **1998**, *109*, 6264.

(29) Amos, R. D.; Alberts, I. L.; Andrews, J. S.; Colwell, S. M.; Handy, N. C.; Jayatilaka, D.; Knowles, P. J.; Kobayashi, R.; Koga, N.; Laidig, K. E.; Maslen, P. E.; Murray, C. W.; Rice, J. E.; Sanz, J.; Simandiras, E. D.; Stone, A. J.; Su, M.-D. CADPAC, The Cambridge Analytic Derivatives Package, Issue 6, Cambridge 1995.

(30) (a) Hohenberg, P.; Kohn, W. *Phys. Rev.* **1964**, *B864−B871*, 136. (b) Kohn, W.; Sham, L. *J. Phys. Rev.* **1965**, *A1133-A1138*, 140. (c) Slater, J. C. In *Quantum Theory of Molecules and Solids. Vol. 4: The Self-Consistent Field for Molecular and Solids*; McGraw-Hill: New York, 1974.

(31) Vosko, S. H.; Wilk, L.; Nusair, M. *Can. J. Phys.* **1980**, *58*, 1200.

(32) Lee, C.; Yang, W.; Parr, R. G. *Phys. Rev. B* **1988**, *37*, 785.

(33) Perdew, J. P. In *Electronic Structure of Solids*; Ziesche, P., Eschrig, H., Eds.; Akademie Verlag: Berlin, 1991; p 11.

(34) Adamo, C.; Barone, V. *Chem. Phys. Lett.* **1997**, *274*, 242.

(35) Perdew, J. P. *Phys. Rev. B* **1986**, *33*, 8822.

(36) Becke, A. D. *J. Chem. Phys.* **1997**, *107*, 8554.

(37) These products are labeled E−1c, E−2c, E−3c$_1$, and E−4c$_1$. The Cartesian coordinates of the optimized geometries are given in the Supporting Information.